Planta (2014) 239:1079–1090
DOI 10.1007/s00425-014-2037-y

ORIGINAL ARTICLE

Analysis of lignin–carbohydrate and lignin–lignin linkages after hydrolase treatment of xylan–lignin, glucomannan–lignin and glucan–lignin complexes from spruce wood

Xueyu Du · Marta Pérez-Boada · Carmen Fernández · Jorge Rencoret · José C. del Río · Jesús Jiménez-Barbero · Jiebing Li · Ana Gutiérrez · Angel T. Martínez

Received: 18 November 2013 / Accepted: 27 January 2014 / Published online: 15 February 2014

Abstract Xylan–lignin (XL), glucomannan–lignin (GML) and glucan–lignin (GL) complexes were isolated from spruce wood, hydrolyzed with xylanase or endoglucanase/β-glucosidase, and analyzed by analytical pyrolysis and 2D-NMR. The enzymatic hydrolysis removed most of the polysaccharide moieties in the complexes, and the lignin content and relative abundance of lignin–carbohydrate linkages increased. Analytical pyrolysis confirmed the action of the enzymatic hydrolysis, with strong decreases of levoglucosane and other carbohydrate-derived products. Unexpectedly it also revealed that the hydrolase treatment alters the pattern of lignin breakdown products, resulting in higher amounts of coniferyl alcohol. From the anomeric carbohydrate signals in the 2D-NMR spectra, phenyl glycoside linkages (undetectable in the original complexes) could be identified in the hydrolyzed GML complex. Lower amounts of glucuronosyl and benzyl ether linkages were also observed after the hydrolysis. From the 2D-NMR spectra of the hydrolyzed complexes, it was concluded that the lignin in GML is less condensed than in XL due to its higher content in β-*O*-4′ ether substructures (62 % of side chains in GML vs 53 % in XL) accompanied by more coniferyl alcohol end units (16 vs 13 %). In contrast, the XL lignin has more pinoresinols (11 vs 6 %) and dibenzodioxocins (9 vs 2 %) than the GML (and both have ~13 % phenylcoumarans and 1 % spirodienones). Direct 2D-NMR analysis of the hydrolyzed GL complex was not possible due to its low solubility. However, after sample acetylation, an even less condensed lignin than in the GML complex was found (with up to 72 % β-*O*-4′ substructures and only 1 % pinoresinols). The study provides evidence for the existence of structurally different lignins associated to hemicelluloses (xylan and glucomannan) and cellulose in spruce wood and, at the same time, offers information on some of the chemical linkages between the above polymers.

Keywords Spruce wood · *Picea abies* · Lignin–carbohydrate complexes (LCCs) · Enzymatic hydrolysis · Analytical pyrolysis · 2D-NMR · Lignin structure

Abbreviations

GL	Glucan–lignin
GML	Glucomannan–lignin
XL	Xylan–lignin
LCC	Lignin–carbohydrate complex
Py-GC/MS	Pyrolysis–gas chromatography/mass spectrometry
2D-NMR	Two-dimensional nuclear magnetic resonance spectroscopy
HSQC	Heteronuclear single quantum coherence
MWL	Milled wood lignin
Ara	Arabinose
Xyl	Xylose
Man	Mannose
Gal	Galactose
Glc	Glucose

X. Du · J. Li (✉)
Department of Fibre and Polymer Technology, Royal Institute of Technology, KTH, Teknikringen 56-58, 10044 Stockholm, Sweden
e-mail: jbing@kth.se

M. Pérez-Boada · C. Fernández · A. T. Martínez
Centro de Investigaciones Biológicas, CSIC, Ramiro de Maeztu 9, 28040 Madrid, Spain

J. Rencoret · J. C. del Río · J. Jiménez-Barbero · A. Gutiérrez
Instituto de Recursos Naturales y Agrobiología de Sevilla, CSIC, PO Box 1052, 41080 Seville, Spain

Introduction

Cellulose, lignin, and hemicelluloses are the three major components of lignocellulosic materials. Between the lignin and the two carbohydrates, chemical linkages are present natively. Although these linkages exist in small amounts, almost all wood lignin is associated with polysaccharides (Du et al. 2013). The linkage types and numbers are still not well understood, although they can cause technical difficulties during processing of lignocellulosic materials, limiting the separation of lignin and carbohydrates in chemical pulping (Iverson and Wannström 1986; Choi et al. 2007) or bioethanol production (Choi et al. 2007; Iverson and Wannström 1986). Therefore, investigation of the structure of native lignin–carbohydrate complexes (LCCs) is of both theoretical and practical importance.

It is generally accepted that there are three types of lignin–carbohydrate linkages present in wood, namely phenyl glycosides, esters, and benzyl ethers (Fengel and Wegener 1984) (Fig. 1). In spruce wood, the most important forestry resource in Sweden, the existence of both benzyl ether and ester bonds has been suggested (Eriksson et al. 1980). Ester bonds were proposed between the 4-*O*-methylglucuronic acid side chains in xylan and the benzylic (C_α) position in lignin units (Eriksson et al. 1980), while the benzyl ether bonds would occur between the same lignin position and primary hydroxyls in hexopyranoses/arabinofuranose or xylose C_2/C_3 secondary hydroxyls, as shown in spruce chemical pulp (Choi et al. 2007). In addition, phenyl glucoside structures have been suggested based on the observation of phenolic content increase after mild acid incubation of spruce wood LCC (Lawoko 2005). Obviously, more reliable investigations on the LCC structures existing in spruce wood are still needed.

For detailed structural investigations, isolation of the LCCs as chemically unaltered as possible is a prerequisite. In addition, sensitive characterization methods are demanded since the quantities of the linkages are small. Recently, an LCC fractionation protocol, universally applicable for native and processed plant biomass, has been developed at KTH (Du et al. 2013). This protocol includes sample disintegration by mild (for structural preservation) ball milling, followed by complete dissolution before fractionation into several LCCs with quantitative recovery. The structural preservation and complete recovery yield guarantee the accuracy and representativeness of the subsequent characterization. From spruce wood, three LCC types were obtained: glucan–lignin (GL), glucomannan–lignin (GML), and xylan–lignin (XL). These fractions differ in their carbohydrate moieties and lignin contents, but the eventual differences in the lignin present in each of them, as well as the nature of the lignin–carbohydrate linkages, are still to be revealed.

In terms of structural characterization, modern solution-state NMR has been proven as one of the most direct and informative techniques (Ralph and Landucci 2010), especially when the instrument is equipped with a cryogenic probe that strongly enhances the detection sensitivity (Kovacs et al. 2005). Using high-resolution NMR, phenyl glycoside, γ-ester and benzyl ether structures have been reported in pine and several hardwoods (Balakshin et al. 2011; Yuan et al. 2011; Miyagawa et al. 2013). Previously, the position of glucuronosyl esters at the lignin γ-position (instead of the benzylic position) had been shown by NMR (Balakshin et al. 2007) in agreement with uronosyl group migration shown by Li and Helm (1995). However, the first attempts to combine fractionation of spruce LCCs with solution-state NMR analysis were unsuccessful (Du et al. 2013). First, only XL, the smallest molecular weight fraction, could be dissolved in NMR solvents, while the two other fractions were either partially or completely insoluble. Second, no lignin–carbohydrate linkage signals could be observed even for the soluble XL fraction. In a similar way, no detailed lignin interunit linkages could be identified to date in the spruce LCCs spectra, which only included barely detectable lignin aromatic signals (together with carbohydrate signals). The difficulties in the NMR analysis of spruce LCCs result from their high molecular weight, due to the presence of linked polysaccharide chains that negatively affect the spin–spin relaxation time (T_2) (Zhang and Gellerstedt 2007).

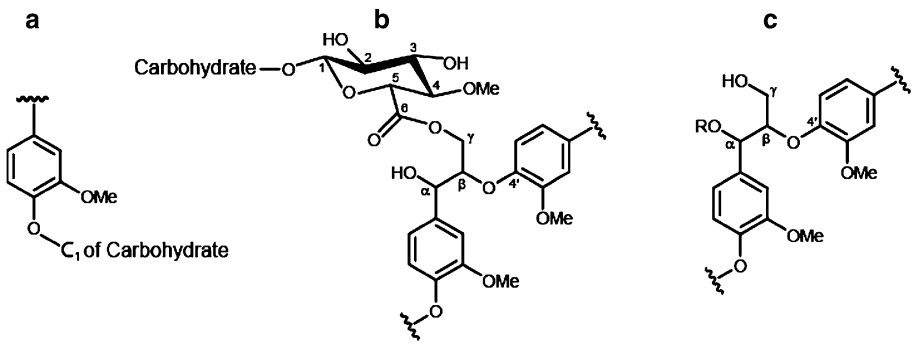

Fig. 1 Three types of lignin–carbohydrate linkages in wood: **a** phenyl glycoside, **b** ester of 4-*O*-methylglucuronic acid on lignin C_γ; **c** benzyl ether, with different sugar units linked on lignin C_α ($R = C_6$ in Glc, Man, Gal, or C_5 in Ara). Adapted from Balakshin et al. (2011)

In the present study, an optimized enzymatic hydrolysis of each spruce wood LCC fraction obtained by Du et al. (2013) was conducted to reduce their molecular weights. Removal of the polysaccharide chains will exert a beneficial effect on sample dissolution, and will also shorten T_2 for improving NMR analysis. At the same time, the samples will be enriched in lignin, and especially in the relative abundance of lignin–carbohydrate linkages, favoring their analysis in the different LCCs. Then, two sensitive analytical approaches were applied for characterization of the enzymatically hydrolyzed LCCs: (1) Pyrolysis-gas chromatography/mass spectrometry (Py-GC/MS); and (2) Heteronuclear single quantum correlation (HSQC) 2D-NMR (using a 600 MHz instrument equipped with cryogenic probe).

Materials and methods

Spruce wood LCC fractions, enzymes and chemicals

GL, GML and XL fractions from spruce (*Picea abies*) wood chips were prepared as reported by Du et al. (2013). Milled-wood lignin (MWL) was also isolated as a reference lignin (Björkman 1956). Cellulolytic enzymes, NS 22086 with high endoglucanase activity and NS 188 with high β-glucosidase activity, and xylanase (NS 51115) were supplied by Novozymes. All chemicals of AR grade were purchased from Fisher Scientific or Sigma.

Enzymatic hydrolysis and general analyses of LCC fractions

200 mg GL or GML was incubated with 1 ml NS 22086 and 0.5 ml NS 188 at 50 °C in 8.5 ml of 0.1 M phosphate (pH 6.0) under continuous shaking. The supernatant was collected and replaced with fresh enzyme and buffer every 24 h until no increase of total released (reducing) sugars, determined using the dinitrosalicylic acid assay (Miller 1959), was detected (72 h incubation time). The hydrolyzed residue was then thoroughly washed by deionized water and freeze dried. 100 mg XL was incubated with 500 µl NS 51115 at 50 °C in 4.5 ml of 0.1 M phosphate (pH 6.0), and the hydrolysis process was continued as described above for the GL and GML treatments. The initial and treated LCC fractions were dissolved in 0.1 M sodium hydroxide and analyzed by size exclusion chromatography (SEC) using three TSK gel columns (3000, 4000 and 3000PW) (Tosoh Bioscience, http://www.tosohbioscience.com) coupled in series, with 0.1 M sodium hydroxide as the eluent. The flow rate was 1 ml min^{-1}, and a Waters 2487 UV detector (http://www.waters.com) was used at 280 nm for detection. The columns were calibrated using polyethylene glycol and polyethylene oxide standards, with specific molecular masses ranging from 0.2 to 250 kDa.

The carbohydrate composition of the treated/untreated LCCs was analyzed according to Theander and Westerlund (1986). Before the enzymatic treatment, Klason lignin was determined according to T222 om-88 (TAPPI test methods 2006–2007. Tappi Press, Norcross, USA), and total carbohydrate was calculated by difference (100-Klason lignin) (Du et al. 2013). After enzymatic hydrolysis, the carbohydrate content was derived from the sum of monosaccharides, and the lignin content (%) was calculated by difference (100-carbohydrate).

The hydrolyzed LCCs were also dissolved in dimethylsulfoxide (DMSO)/*N*-methylimidazole (2:1, v/v, 4.5 ml) at room temperature for 2 h, and acetylated by adding acetic anhydride (1.5 ml) with further stirring for 2 h at room temperature and then pouring the mixture into distilled water (1 l) to quench the reaction. The resultant precipitate was recovered by filtration, washed with ultrapure water (1 l) and lyophilized to yield acetylated sample, which was dissolved in deuterated chloroform ($DCCl_3$) (750 µl) for NMR experiments.

Py-GC/MS

Approximately 100 µg sample was analyzed with an EGA/PY-3030D micro-furnace pyrolyzer (Frontier Laboratories Ltd.) connected to an Agilent 7820A gas chromatograph using a DB-1701 fused-silica capillary column (60 m × 0.25 mm i.d., 0.25 µm film thickness) and an Agilent 5975 mass selective detector (EI at 70 eV). The pyrolysis was performed at 500 °C for 1 min. The GC oven temperature was elevated from 45 °C (4 min) to 280 °C (10 min) with the heating rate of 4 °C/min. Helium was served as the carrier gas (2 ml/min).

HSQC 2D-NMR analysis

For NMR experiments, 20 mg of the initial or the enzymatically treated LCCs were dissolved in 0.75 ml of deuterated DMSO-d_6 or $DCCl_3$ in the case of acetylated samples. NMR spectra were recorded at 25 °C on a Bruker AVANCE 600 MHz instrument equipped with a cryogenically cooled z-gradient triple-resonance probe. HSQC experiments used Bruker's 'hsqcetgp' pulse program generally with spectral widths of 5,000 and 13,200 Hz for the ^{1}H- and ^{13}C-dimensions. The number of collected complex points was 2,048 for the ^{1}H-dimension with a recycle delay of 1 s. The number of transients was 64, and 256 time increments were recorded in ^{13}C-dimension. The $^{1}J_{CH}$ used was 140 Hz. The *J*-coupling evolution delay was set to 3.2 ms. Processing used typical matched Gaussian apodization in ^{1}H and a squared cosine-bell in ^{13}C. Prior to Fourier transformation,

the data matrices were zero filled up to 1,024 points in the ^{13}C-dimension. The central DMSO (δ_C/δ_H 39.5/2.49 ppm) and chloroform (δ_C/δ_H 77.0/7.26 ppm) peaks were used as internal references. Integration of HSQC cross-signals was performed separately for the different regions of the HSQC spectrum, which contains signals that correspond to chemically analogous carbon–proton pairs. For these signals, the $^1J_{CH}$ coupling value is similar and integrals can be used semiquantitatively to estimate the relative abundance of the different species. In the aliphatic oxygenated region, the relative abundances of side chains involved in interunit linkages or present in terminal units were estimated from the C_α–H_α correlations to avoid possible interference from homonuclear ^{1}H–^{1}H couplings. The LCC linkages were semiquantitatively estimated from their specific signals described later.

Results and discussion

Separation of spruce LCCs

Three different LCCs (GL, GML and XL) were isolated from spruce wood with 93 % total recovery (Du et al. 2013). As shown in Table 1, GL is a glucan-based polymer (86 % of monosaccharides being glucose) with 19 % lignin. GML is mainly composed of glucose and mannose (49 and 31 % of monosaccharides, respectively) with 29 % lignin. XL is a xylose-enriched polymer (65 % of monosaccharides) with 43 % lignin. Other sugars (with abundance >10 %) are xylose in GML, and glucose/arabinose in XL. Considering the recovery of the three fractions (50, 31 and 13 %, respectively), it is possible to establish the following material balance for the initial lignin (27 % Klason lignin in wood): 35 % in GL, 33 % in GML and 20 % in XL. Previous studies on these LCCs (Du et al. 2013) revealed the existence of chemical linkages between the lignin and the carbohydrate moieties. These studies also showed that the high carbohydrate contents are behind the high molecular weights of these LCCs, 490 kDa (GL), 63–160 kDa (GML) and 18 kDa (XL), respectively.

For reliable investigation of LCC structures, modern 2D NMR should be highly preferred. However, there were some difficulties for dissolving the LCC fractions in common NMR solvents, except for XL that could be dissolved in DMSO-d_6. GML exhibited some solubility, but far from the level required for analysis, and GL was completely insoluble. Moreover, the quality of the spectra obtained was low, even in the case of XL, due to the high molecular weight.

Enzymatic hydrolysis of spruce LCCs

Since the main focus of the structural analysis lays on the lignin part of the LCCs, including the lignin–carbohydrate linkages, extensive enzymatic hydrolysis of the polysaccharide chains was performed to improve the NMR analysis. Due to the specificity of the carbohydrate enzymes applied, the structure of lignin and the lignin–carbohydrate linkages should be intact, although cleavage of phenyl glycoside linkages by a β-glycosidase containing cellulase cocktail has been reported (Balakshin et al. 2011).

Cellulases have been generally used for lignin isolation from wood and paper pulps (Chang et al. 1975; Ibarra et al. 2004), since cellulose is the major polysaccharide in the plant cell wall. The LCCs obtained from spruce wood have different polysaccharide compositions. Therefore, more specific hydrolyses were performed based on the known sugar composition of each LCC, including cellulase (endoglucanase plus glucosidase) for GL and xylanase for XL. Although lignin-free glucomannan from spruce holocellulose was easily hydrolyzed by commercial mannanase (NS 51023), the enzyme was unable to hydrolyze the GML fraction from spruce wood. Finally, the cellulase formulation showed the highest efficiency in hydrolyzing the GML fraction.

As shown in Table 1, the enzymatic hydrolysis of each LCC fraction was successful, since most of the polysaccharide moieties were effectively degraded and removed, with only 7 % carbohydrate left for GL and GML and 1 % for XL. On the other hand, the lignin content in each hydrolyzed LCC (En-LCC) fraction reached very high levels (all above 90 %). Correspondingly, the molecular masses (M_w)

Table 1 Total carbohydrate and lignin content, and carbohydrate composition (*ara* arabinose, *Xyl* xylose, *Man* mannose, *Glc* glucose, *Gal* galactose) of the spruce wood LCCs before (GL, GML and XL) and after (En-GL, En-GML and En-Xyl) enzymatic hydrolysis

LCC	Carbohydrate (%)	Lignin (%)	Relative carbohydrate composition (%)				
			Ara	Xyl	Man	Glc	Gal
GL	80.7	19.3	1.9	2.5	8.6	85.8	1.2
En-GL	7.1	92.9	9.9	9.9	35.2	18.3	26.8
GML	70.8	29.2	4.7	10.6	30.9	49.4	4.4
En-GML	7.4	92.6	6.8	5.4	44.6	28.4	14.9
XL	57.3	42.7	13.0	65.3	3.2	15.6	3.0
En-XL	1.2	98.8	8.3	8.3	58.3	8.3	16.7

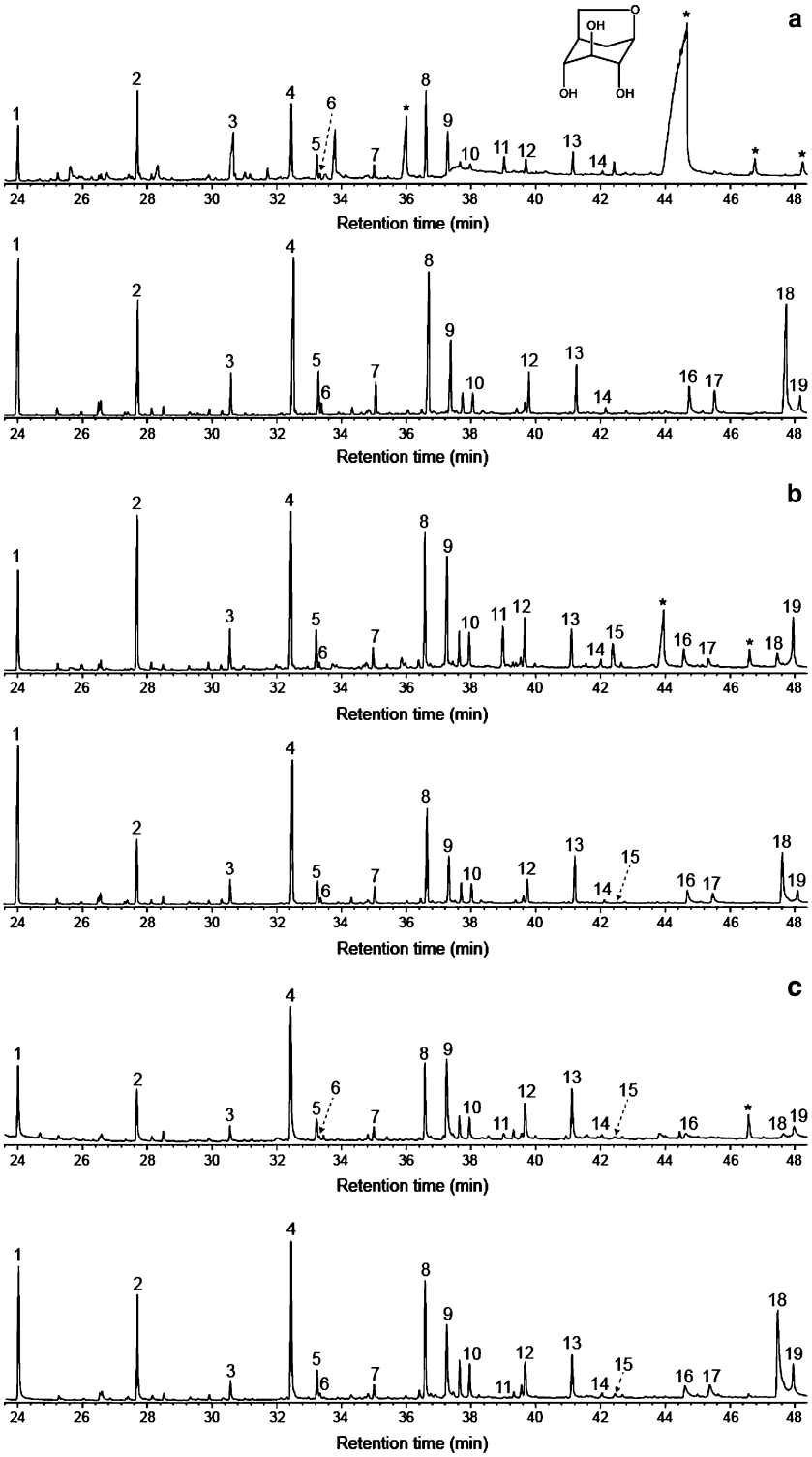

Fig. 2 Pyrograms of GL (**a**), GML (**b**) and XL (**c**) complexes before (*top*) and after (*bottom*) enzymatic hydrolysis, showing the disappearance of levoglucosane (the strongest peak in **a**) and other carbohydrate peaks (*other asterisks*). The identity of the different lignin-derived products is shown in Table 2

dropped to 19.9 kDa (En-GL), 18.7 kDa and 14.6 kDa (En-XL), close to that of the MWL sample (10.9 kDa). This greatly enhanced the solubility in conventional NMR solvents, and would increase the relative abundances of the lignin–carbohydrate and lignin–lignin linkages to be analyzed by NMR, as discussed below.

Py-GC/MS analysis

Py-GC/MS is a useful method to analyze lignin composition, and obtain rough information on the relative lignin-to-carbohydrate content (del Rio et al. 2002). As shown in Fig. 2, nineteen main lignin-derived compounds

Table 2 Relative abundances (peak areas) of the main lignin-derived products from Py-GC/MS (Fig. 2) of the spruce LCCs before (GL, GML and XL) and after (En-GL, En-GML and En-XL) enzymatic hydrolysis, and wood MWL

		Relative peak areas						
		MWL	GL	En-GL	GML	En-GML	XL	En-XL
1	Guaiacol	14.1	14.5	18.9	11.1	26.9	13.5	16.0
2	4-Methylguaiacol	9.8	19.0	10.7	16.1	8.1	8.8	10.5
3	4-Ethylguaiacol	2.2	2.7	3.2	4.1	2.9	2.4	2.0
4	4-Vinylguaiacol	11.3	16.4	14.7	14.9	17.8	20.9	15.9
5	Eugenol	2.2	4.7	3.2	3.3	2.5	2.9	2.2
6	4-Propylguaiacol	0.3	1.0	0.7	0.4	0.5	0.2	0.3
7	Isoeugenol (*cis*)	1.4	2.6	2.2	1.8	1.8	1.8	1.2
8	Isoeugenol (*trans*)	8.1	17.1	12.6	11.8	10.8	10.6	10.2
9	Vanillin	11.0	8.8	6.6	10.9	5.6	14.5	7.7
10	4-Propynylguaiacol	1.2	1.1	1.4	2.9	2.1	3.1	3.0
11	Homovanillin	2.3	3.9	0	4.0	0	0.9	0.1
12	Acetoguaiacone	4.8	3.1	3.0	4.4	2.5	5.9	3.5
13	Guaiacyl acetone	1.5	4.5	3.5	3.4	4.9	7.8	4.4
14	Propioguaiacone	0.4	0.8	0.4	0.5	0.3	0.6	0.5
15	Guaiacyl vinyl ketone	1.9	0	0	1.4	0.1	0.4	0.4
16	Dihydroconiferyl alcohol	2.8	0	3.2	2.4	2.7	1.5	2.4
17	Coniferyl alcohol (*cis*)	2.5	0	2.5	0.9	2.0	0.0	2.3
18	Coniferyl alcohol (*trans*)	13.3	0	11.9	1.8	7.3	0.8	14.4
19	Coniferaldehyde	8.8	0	1.3	3.9	1.2	3.1	3.0

were obtained by Py-GC/MS of the initial and enzymatically hydrolyzed spruce LCCs and MWL, whose identities and relative abundances are provided in Table 2. The initial pyrograms also contained carbohydrate-derived products, being especially abundant in the GL pyrogram, which includes a strong peak of levoglucosane from glucose pyrolysis (Fig. 2). Interestingly, after the hydrolysis treatment the carbohydrate peaks were almost completely removed showing the efficiency of the enzymatic hydrolysis.

Comparing the relative composition of the pyrolysis products from the initial and the enzymatically hydrolyzed LCCs, some differences could be observed. The most significant difference concerns coniferyl alcohol, whose total relative abundance (*cis* and *trans* isomers) in the initial LCCs was very low (0 % in GL, 3 % in GML, and 1 % in XL), but it significantly increased after the enzymatic hydrolysis attaining "normal" values (14 % in GL, 9 % in GML and 17 % in XL) similar to those found from MWL (16 %). This shows that the presence of carbohydrates influences the pyrolytic degradation of lignin in LCCs. Coniferyl alcohol is formed by alkyl-aryl ether breakdown and side chain dehydration in lignin units (Nakamura et al. 2008), which in spruce often present a C_α hydroxyl and a C_β-ether linkage. Therefore, the results obtained suggest that the presence of linkages to carbohydrates in the lignin side chains (or maybe also at the C_4 position of the aromatic ring) prevents the above degradation/dehydration reaction, and no coniferyl alcohol is formed during Py-GC/MS. In any case, the results obtained reveal for the first time that the presence of carbohydrates in LCCs can influence the pyrolytic breakdown pattern, including a strong reduction of coniferyl alcohol among the lignin-derived products.

2D-NMR analysis: lignin–carbohydrate linkages

2D NMR is a powerful tool for analyzing both lignin–lignin and lignin–carbohydrate linkages. The HSQC NMR spectra of the hydrolyzed GML, XL and GL fractions (in DMSO-d_6) are shown in Figs. 3a, b and 4a, respectively, and the assignments of the main lignin, and carbohydrate anomeric signals are included in Table 3.

According to Balakshin et al. (2011), phenyl glycoside, uronic γ-ester and benzyl ether lignin–carbohydrate linkages (Fig. 1) can be identified in LCCs from characteristic 2D NMR cross-signals (see Table 4, last column), which were assigned based on previous studies with model compounds (Toikka and Brunow 1999; Toikka et al. 1998; Tokimatsu et al. 1996; Terashima et al. 1996; Li and Helm 1995). None of the above signals could be observed in the HSQC spectra of the spruce LCC fractions before the enzymatic hydrolysis, due to the low relative abundance of the lignin–carbohydrate linkages and the poor quality of the spectra. Notably, the above difficulties were apparently solved by the enzymatic hydrolysis of the XL and GML

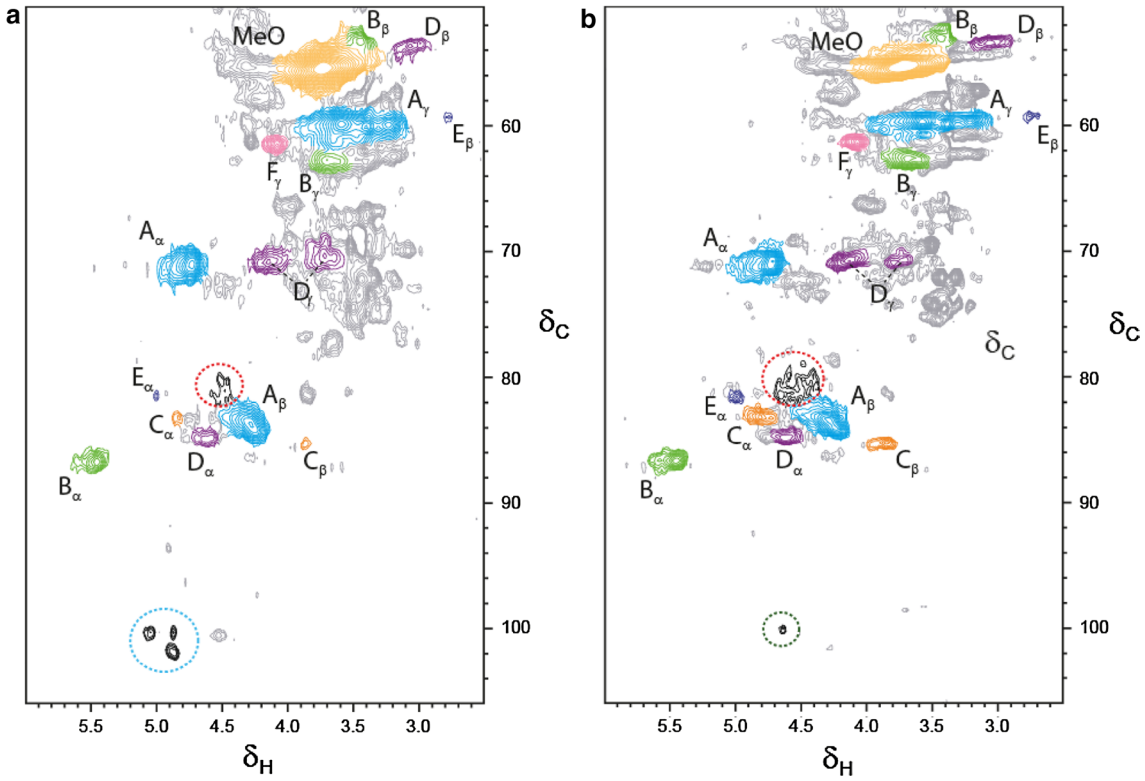

Fig. 3 HSQC spectra of spruce GML (**a**) and XL (**b**) complexes after enzymatic hydrolysis (DMSO-d_6 as solvent). Aliphatic oxygenated region (δ_C/δ_H 50–105/2.5–6 ppm) showing correlation signals from main lignin substructures (**a**–**f** in Fig. 6). *Circles* indicate some lignin–carbohydrate linkages described in the text (and Fig. 5)

fractions, since new signals related to the lignin–carbohydrate linkages mentioned above appeared in the HSQC spectra (Fig. 3). However, the GL spectrum was still not enough resolved after the enzymatic hydrolysis (Fig. 4a) and no signals could be assigned to lignin–carbohydrate linkages (although its lignin moiety could be analyzed after sample acetylation, as described below).

First, the disappearance of the carbohydrate anomeric signals (Table 3) and the appearance of possible lignin–carbohydrate signals after the enzymatic treatment were observed. This is better shown in Fig. 5, which provides a detail of the δ_C/δ_H 95–110/4–5.5 ppm region of the HSQC spectra of GML (top) and XL (bottom) before (left) and after (right) the enzymatic hydrolysis. The marked signals were not observed in the spectrum of the carbohydrate-free MWL isolated from spruce wood (spectrum not shown) confirming that they originated from substituted sugars. The circled signals observed in the treated GML spectrum (Fig. 5b) probably correspond to phenyl glycoside linkages, as reported by Balakshin et al. (2011) based on monolignol glycoside data (Terashima et al. 1996) (Table 4). Although the existence of phenyl glucoside structures has been suggested in spruce wood LCC (Lawoko 2005), no direct proof has been described in spruce lignin to date. There are three of such signals in the spectrum of hydrolyzed GML, probably implying the involvement of three different types of sugar units forming glycosidic-type linkages with phenolic hydroxyls in lignin. The abundance of the above phenyl glycoside linkages could be underestimated in the present study due to partial cleavage during the LCC treatment with the different hydrolases used (Balakshin et al. 2011). Several phenyl glycoside signals have also been reported in LCCs from different woods (Miyagawa et al. 2013; Yuan et al. 2011; Balakshin et al. 2011). In the spectrum of the hydrolyzed XL, only one small signal was observed in the neighbor region being tentatively assigned to esterified 4-*O*-methylglucuronic acid (Fig. 5d). This uronic acid would be present acylating the lignin side chains (Balakshin et al. 2007; Li and Helm 1995). However, in contrast to that reported by Balakshin et al. (2011), the complementary side chain signal was not observed in the δ_C/δ_H 62–65/4.0–4.5 ppm region of the spectrum, most probably because of its low intensity and signal overlapping (Fig. 3b). The latter signal is especially difficult to be assigned when lignin is γ-esterified with other acids, as in the poplar LCCs analyzed by Yuan et al. (2011). However, the present LCC isolation method would be problematic

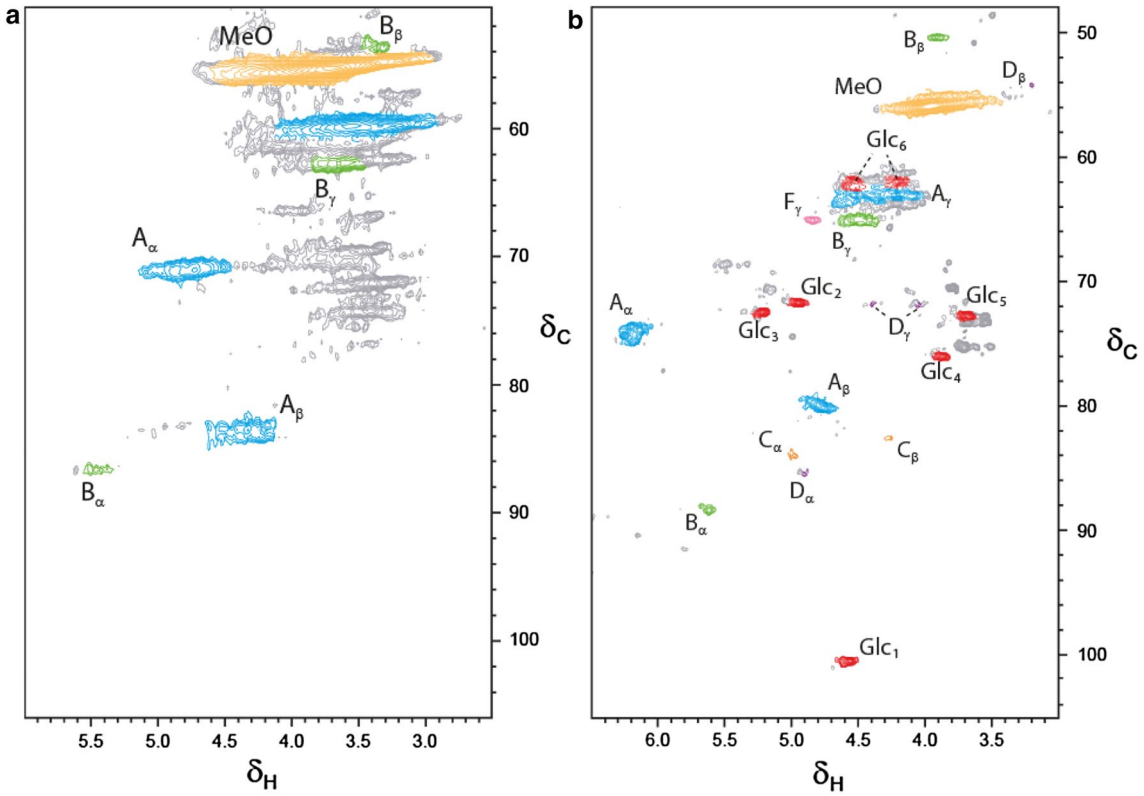

Fig. 4 HSQC spectra of enzymatically hydrolyzed spruce GL complex before (**a**) and after acetylation to improve solubility (**b**) (in DMSO-*d6* and $DCCl_3$, respectively). Aliphatic oxygenated region (δ_C/δ_H 50–105/2.5–6 ppm) showing correlation signals from main lignin substructures (**a**–**f** in Fig. 6). C_1–H_1 to C_6–H_6 correlation signals in acetylated β-D-glucopyranoside units (Glc_1 to Glc_6) are also shown in **b**

for analyzing LCC ester linkages since they can be hydrolyzed under the alkaline conditions used.

Although the existence of two types of benzyl ether lignin–carbohydrate linkages has been reported (Choi et al. 2007), one of the NMR signals (δ_C/δ_H 80–81/4.9–5.1 ppm) would overlap with the $^{13}C_\alpha$–$^{1}H_\alpha$ correlation in spirodienones (structure **E** in Fig. 6) (Balakshin et al. 2011; Miyagawa et al. 2013). Therefore, only another benzyl ether structure (at δ_C/δ_H 80–81/4.5–4.7 ppm) was tentatively assigned in the hydrolyzed spruce LCCs (Fig. 3) that, according to the literature, would correspond to the C_α-position of lignin etherified to primary hydroxyls of glucose, galactose, mannose or arabinose units (Table 4). However, in contrast to that observed for the three phenyl glycoside (and the lignin uronate) signals, the broad δ_C/δ_H 80–81/4.5–4.7 ppm signal was also observed in the non-hydrolyzed GML and XL complexes. Furthermore, in agreement with the NMR studies of other LCCs (Miyagawa et al. 2013; Yuan et al. 2011; Balakshin et al. 2011), no signal of benzyl ester bonds, at δ_C/δ_H 75–77/6.0–6.2 ppm (Li and Helm 1995), was found. The results from semiquantitative quantification of the above signals of lignin–carbohydrate linkages in GML and XL are included in Table 4.

Although the exact sugar units involved in the phenyl glycoside and benzyl ether linkages require further investigation, the monosaccharide composition of the enzymatically treated LCCs might supply some clues. As shown in Table 1, mannose and galactose are two of the main polysaccharide units after the LCC enzymatic treatment. Although the abundance of mannose could also be related to a low mannosidase activity of the enzymatic preparations, its involvement in lignin linkages (or in neighbor positions to the lignin-linked sugar units) can be considered, taking into account its predominance in the three hydrolyzed complexes. Interestingly, a strong increase of galactose over constructing sugars (i.e., glucose, mannose and xylose in GL, GML and XL, respectively) was observed (e.g., the Gal/Man ratio moved from 1:8 in the initial GML to 1:3 after the hydrolysis treatment). Therefore, the galactose side chains of the galactoglucomannan polymer would be involved in the lignin–carbohydrate linkages, as reported also for the 4-*O*-methylglucuronic side chains of xylan. Moreover, both mannose and galactose units have been reported to participate in benzyl ether lignin–carbohydrate linkages in spruce chemical pulps (Choi et al. 2007).

Table 3 Assignment of main ^{13}C–^{1}H correlation signals from lignin side chains (in original and acetylated samples), and carbohydrate anomeric signals, in the HSQC spectra of Figs. 3, 4, 5

Label	δ_C/δ_H (ppm)	Assignment
Lignin side chain signals (in DMSO-d_6)		
B_β	53.0/3.45	C_β–H_β in phenylcoumaran substructures
D_β	53.6/3.07	C_β–H_β in resinol substructures
E_β	59.3/2.77	C_β–H_β in spirodienone substructures
A_γ	59.8/(3.24, 3.61)	C_γ–H_γ in β-*O*-4′ substructures
C_γ	60.1/3.41	C_γ–H_γ in dibenzodioxocin substructures
Fγ	61.4/4.06	C_γ–H_γ in cinnamyl alcohol end groups
B_γ	62.7/3.71	C_γ–H_γ in phenylcoumaran substructures
D_γ	70.9/(3.74, 4.15)	C_γ–H_γ in resinol substructures
A_α	71.0/4.74	C_α–H_α in β-*O*-4′ substructures
E_α	81.7/5.03	C_α–H_α in spirodienone substructures
C_α	83.3/4.83	C_α–H_α in dibenzodioxocin substructures
A_β	83.9/4.28	C_β–H_β in β-*O*-4′ substructures
D_α	85.0/4.65	C_α–H_α in resinol substructures
C_β	85.4/3.86	C_β–H_β in dibenzodioxocin substructures
B_α	87.0/5.46	C_α–H_α in phenylcoumaran substructures
Lignin side chain signals (acetylated samples, in $CDCl_3$)		
B_β	50.4/3.90	C_β–H_β in phenylcoumaran substructures
D_β	54.2/3.19	C_β–H_β in resinol substructures
A_γ	62.0/4.20 and 4.52	C_γ–H_γ in β-*O*-4′ substructures
Fγ	65.0/4.83	C_γ–H_γ in cinnamyl alcohol end groups
B_γ	65.0/4.89	C_γ–H_γ in phenylcoumaran substructures
D_γ	71.8/4.03 and 4.38	C_γ–H_γ in resinol substructures
A_α	74.1/6.19	C_α–H_α in β-*O*-4′ substructures
A_β	80.1/4.76	C_β–H_β in β-*O*-4′ substructures
C_β	82.5/4.26	C_β–H_β in dibenzodioxocin substructures
C_α	84.0/5.00	C_α–H_α in dibenzodioxocin substructures
D_α	85.2/4.26	C_α–H_α in resinol substructures
B_α	88.4/5.62	C_α–H_α in phenylcoumaran substructures
Carbohydrate anomeric signals (C_1–H_1; in DMSO-d_6)		
$GlcA_1$	99.2/5.08	4-*O*-Methyl-α-D-glucuronic acid
Man_1	100.4/4.53	(1 → 4)-β-D-Mannopyranoside
Xyl_1	101.71/4.26	β-D-Xylopyranoside
Glc_1	102.7/4.31	(1 → 4)-β-D-Glucopyranoside
Gal_1	105.2/4.26	(1 → 4)-β-D-Galactopyranoside
Ara_1	107.0/5.35	α-L-Arabinofuranoside
$Ara_{1(t)}$	107.9/4.76	α-L-Arabinofuranoside (terminal)

2D-NMR analysis: lignin interunit linkages

The enzymatic removal of most (over 90 %) of the carbohydrate moiety from the spruce LCCs not only enabled the detection of lignin–carbohydrate linkages, but also yielded highly enriched (93–99 % pure) lignin preparations with improved solubility properties. This resulted in a remarkable improvement of the intensity of the lignin signals in the 2D-NMR spectra of hydrolyzed GML and XL complexes. In this way, five main interunit linkages in softwood lignin (Fig. 6), i.e., β-*O*-4′ ether (**A**), phenylcoumaran (β-5′; **B**), dibenzodioxocin (5′-5″-α-*O*-4′/β-*O*-4″; **C**) pinoresinol (β-β′/α-*O*-γ′/α′-*O*-γ; **D**), and spirodienone (β-1′/α-*O*-α′; **E**), and the coniferyl alcohol end units (**F**), could be clearly identified in the spectra of the hydrolyzed GML (Fig. 3a) and XL (Fig. 3b). The assignments of the different NMR signals from the above lignin structures based on previous studies (Du et al. 2013; Ralph and Landucci 2010; Rencoret et al. 2009; Zhang et al. 2006) are listed in Table 3.

As already mentioned, the spectrum of the enzymatically hydrolyzed GL (Fig. 4) was not resolved enough, except for the signals originated from the β-*O*-4′ and phenylcoumaran linkages, and the methoxyl groups of lignin, due to its still low solubility in DMSO-d_6. However, this GL sample could be analyzed after acetylation yielding an NMR spectrum (in $CDCl_3$) with well resolved lignin and polysaccharide signals (Fig. 4b). The intensity of the polysaccharide (glucan) signals was comparatively low, indicating that the low solubility before GL acetylation was not due to a very high polysaccharide content. The same lignin signals identified in the GML and XL spectra could be assigned although with modified chemical shifts due to the presence of acetyl groups (Table 3), together with the different signals from the residual acetylated glucan (Glc_1 to Glc_6 in Fig. 4b). No new information was provided by 2D NMR of the other acetylated LCCs (spectra not shown).

To compare the relative percentage of the different lignin substructures in the spruce LCCs, the signals originated from the C_α position of the lignin side chains in the spectra of hydrolyzed GML and XL and acetylated hydrolyzed GL were integrated (since they are easily recognized without overlapping with other signals). Spruce MWL was taken as a reference to identify the signals (spectrum not shown) and for lignin composition comparison. Moreover, quantitative ^{13}C NMR analysis of carbonyl/carboxyl functionalities in this lignin (spectrum not shown) only showed traces (always <0.5 % of total carbon) of Cα-oxidized β-*O*-4′ and aryl aldehyde structures at 194 and 191 ppm, respectively.

β-*O*-4′ ethers (53–72 % of side chains) and phenylcoumarans (11–17 %) are the main substructures in spruce lignin, together with coniferyl alcohol end groups (8–16 %) as shown by the HSQC spectra of MWL and LCCs (Table 5), followed by smaller percentages of pinoresinols (1–11 %) and dibenzodioxocins (2–9 %) and the smallest amounts of spirodienones (≤1 %). When the LCCs are compared, the GL lignin appeared as the most different, with the highest amount of β-*O*-4′ ethers (72 %), the lowest amount of pinoresinols (1 %) and the absence of spirodienones. The opposite was observed for the XL lignin with the highest amounts of pinoresinols

Table 4 Assignment and semiquantitative quantity estimation of main ^{13}C–^{1}H correlation signals of lignin–carbohydrate linkages in the HSQC spectra (Fig. 6) of the enzymatically hydrolyzed spruce LCCs (En-GML and En-XL) and previous assignment for pine and birch LCCs by Balakshin et al. (2011)

Linkage type	^{13}C–^{1}H correlation	δ_C/δ_H (ppm) (quantity per 100 aromatic units)		
		En-GML	En-XL	Balakshin et al. (2011)
γ-Esters	lignin C_γ	–	–	62–65/4.0–4.5
Benzyl ether	lignin C_α	80–82/4.4–4.6 (3.8)	80–82/4.4–4.7 (6.1)	80–81/4.5–4.7, 4.9–5.1
Esterified GlcA	Sugar C_1	–	100.1/4.62 (0.5)	101/4.7
Phenyl glycoside-1	Sugar C_1	100.2/5.03 (1.5)	–	99–104/4.8–5.2
Phenyl glycoside-2	Sugar C_1	100.3/4.85 (0.8)		
Phenyl glycoside-3	Sugar C_1	101.9/4.86 (2.1)	–	

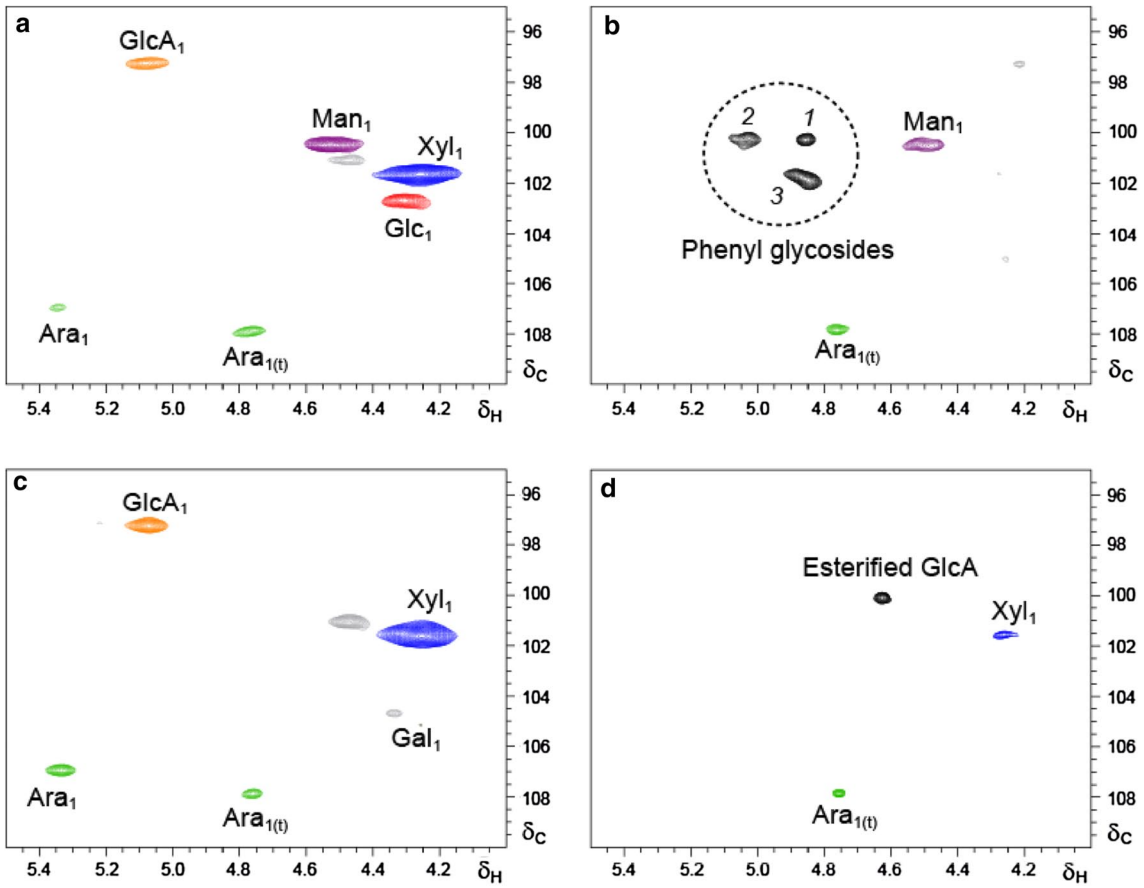

Fig. 5 Details of the carbohydrate anomeric region (δ_C/δ_H 95–110/4–5.5 ppm) in HSQC spectra of spruce GML and XL complexes before (**a**, **c**, respectively) and after (**b**, **d**, respectively) enzymatic hydrolysis of their carbohydrate moieties revealing some lignin–carbohydrate linkages (DMSO-d_6 as solvent)

(11 %) and the lowest amount of β-*O*-4′ ethers (53 %). The latter lignin is the most similar to the spruce MWL (with 53–56 % β-*O*-4′ ethers) although it has less phenylcoumarans and slightly higher dibenzodioxocin and spirodienone contents. Moreover, the MWL differs from the LCC lignins in the lower amounts of coniferyl alcohol end groups (8 vs 13–16 %, respectively). Finally, the GML lignin presents a composition relatively similar to the GL lignin, although with a significant content of pinoresinols (instead of the very low content characteristic of the GL lignin) and less β-*O*-4′ ethers. The XL lignin (and the wood MWL) would have a more condensed structure, with a total of 34 % of side chains forming phenylcoumaran, pinoresinol, dibenzodioxocin or spirodienone linkages. By contrast, the GL lignin would have the most linear

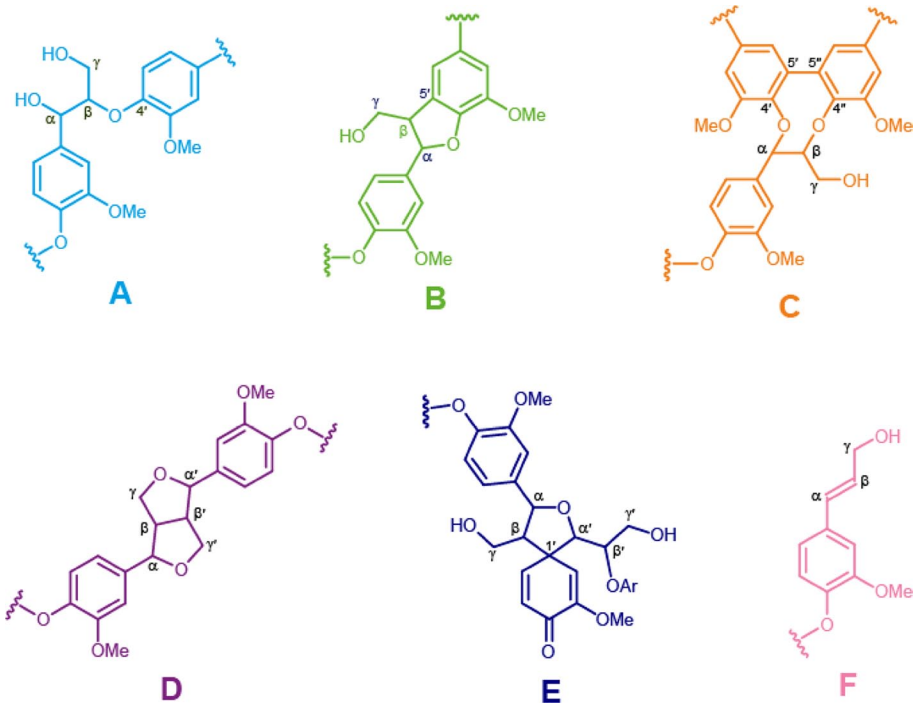

Fig. 6 Main lignin substructures identified in the HSQC spectra (Figs. 3, 4) of spruce LCCs

Table 5 Relative abundance of lignin interunit linkages from HSQC spectra of the enzymatically hydrolyzed LCCs from spruce wood (En-GL, En-GML and En-XL), and wood MWL

	Percentage of side chains			
	MWL	En-GL[a]	En-GML	En-XL
β-*O*-4′ ether (**A**)	56	72	62	53
Phenylcoumaran (**B**)	17	11	14	13
Dibenzodioxocin (**C**)	8	2	2	9
Pinoresinol (**D**)	9	1	6	11
Spirodienone (**E**)	1	0	1	1
Coniferyl alcohol end groups (**F**)	8	14	16	13

[a] From acetylated sample

structure with high predominance of side chains forming β-*O*-4′ ether linkages (72 %) and very low amounts (only 14 %) of other interunit linkages (together with 14 % end groups). The almost near absence of pinoresinols (and the absence of spirodienones) makes GL lignin very different from the other LCC lignins and from the wood MWL. The existence of different lignins in the three LCCs agrees with the preliminary results using thioacidolysis (Du et al. 2013).

Conclusions

Enzymatic hydrolysis could remove most of the carbohydrate structures from the three LCCs obtained from spruce wood, with the hydrolyzed complexes being enriched in lignin and lignin–carbohydrate linkages. Py-GC/MS confirmed the extensive removal of carbohydrates during the enzymatic treatment, and provided new information on the effect on the pyrolytic breakdown pattern of lignin in spruce LCCs. Carbohydrate removal from the LCCs makes their 2D-NMR analysis possible and reveal the linkage differences between the three LCCs. Among them, the lignin linked to xylan was more similar to the reference MWL from wood, while the lignin in the glucan fraction was the most different with a predominance of alkyl-aryl ethers and absence of some condensed substructures. The lignin in the glucomannan fraction presented intermediate characteristics. In spite of some possible drawbacks (related to the eventual cleavage of phenyl glycoside and ester lignin–carbohydrate bonds) the present study provides a new approach to analyze lignins and the linked carbohydrates by combining quantitative fractionation of wood into three LCCs and 2D-NMR analysis after hydrolase treatment, which enriches the samples' relative lignin–lignin and lignin–carbohydrate linkage abundances to facilitate the analysis.

Acknowledgments This study was supported by the EU projects LIGNODECO (KBBE-2009-3-244362), the ProLignin project of the WoodWisdom-Bioenergy ERA-Net, and the Spanish project AGL2011-25379. J.R. thanks the CSIC for a JAE-DOC contract, cofinanced by Fondo Social Europeo. Alicia Prieto (CIB, Madrid) is acknowledged for the monosaccharide analysis of the enzymatically treated LCCs.

References

Balakshin MY, Capanema EA, Chang HM (2007) MWL fraction with a high concentration of lignin-carbohydrate linkages: isolation and 2D NMR spectroscopic analysis. Holzforschung 61:1–7

Balakshin M, Capanema E, Gracz H, Chang HM, Jameel H (2011) Quantification of lignin-carbohydrate linkages with high-resolution NMR spectroscopy. Planta 233:1097–1110

Björkman A (1956) Studies on finely divided wood. Part 1. Extraction of lignin with neutral solvents. Svensk Papperstidn 59:477–485

Chang HM, Cowling EB, Brown W, Adler E, Miksche G (1975) Comparative studies on cellulolytic enzyme lignin and milled wood lignin of sweetgum and spruce. Holzforschung 29:153–159

Choi JW, Choi DH, Faix O (2007) Characterization of lignin-carbohydrate linkages in the residual lignins isolated from chemical pulps of spruce (*Picea abies*) and beech wood (*Fagus sylvatica*). J Wood Sci 53:309–313

del Rio JC, Speranza M, Gutierrez A, Martinez MJ, Martinez AT (2002) Lignin attack during eucalypt wood decay by selected basidiomycetes: a Py-GC/MS study. J Anal Appl Pyrol 64:421–431

Du X, Gellerstedt G, Li J (2013) Universal fractionation of lignin-carbohydrate complexes (LCCs) from lignocellulosic biomass: an example using spruce wood. Plant J 74:328–338

Eriksson Ö, Goring DAI, Lindgren BO (1980) Structural studies on the chemical-bonds between lignins and carbohydrates in spruce wood. Wood Sci Technol 14:267–279

Fengel D, Wegener G (1984) Wood: chemistry, ultrastructure, reactions. Walter de Gruyter, Berlin

Ibarra D, del Rio JC, Gutierrez A, Rodriguez IM, Romero J, Martıinez MJ, Martinez AT (2004) Isolation of high-purity residual lignins from eucalypt paper pulps by cellulase and proteinase treatments followed by solvent extraction. Enzyme Microb Tech 35:173–181

Iverson T, Wannström S (1986) Lignin-carbohydrate bonds in a residual lignin isolated from pine kraft pulp. Holzforschung 40:19–22

Kovacs H, Moskau D, Spraul M (2005) Cryogenically cooled probes—a leap in NMR technology. Prog Nucl Mag Res Sp 46:131–155

Lawoko M (2005) Lignin polysaccharide networks in softwood and chemical pulps: characterisation, structure and reactivity. Royal Institute of Technology, Stockholm

Li K, Helm RF (1995) Synthesis and rearrangement reactions of ester-linked lignin-carbohydrate model compounds. J Agric Food Chem 43:2098–2103

Miller GL (1959) Use of dinitrosalicylic acid reagent for determination of reducing sugar. Anal Chem 31:426–428

Miyagawa Y, Kamitakahara H, Takano T (2013) Fractionation and characterization of lignin-carbohydrate complexes (LCCs) of *Eucalyptus globulus* in residues left after MWL isolation. Part II: analyses of xylan-lignin fraction (X-L). Holzforschung. doi: 10.1515/hf-2012-0148

Nakamura T, Kawamoto H, Saka S (2008) Pyrolysis behavior of Japanese cedar wood lignin studied with various model dimers. J Anal Appl Pyrol 81:173–182

Ralph J, Landucci LL (2010) NMR of lignin. In: Heitner C, Dimmel D, Schmidt J (eds) Lignin and lignans: advances in chemistry. CRC Press, Boca Raton, pp 137–243

Rencoret J, Marques G, Gutierrez A, Nieto L, Ignacio Santos J, Jimenez-Barbero J, Martinez AT, del Rio JC (2009) HSQC-NMR analysis of lignin in woody (*Eucalyptus globulus* and *Picea abies*) and non-woody (*Agave sisalana*) ball-milled plant materials at the gel state. Holzforschung 63:691–698

Terashima N, Ralph SA, Landucci LL (1996) New facile syntheses of monolignol glucosides; *p*-glucocoumaryl alcohol, coniferin, and syringin. Holzforschung 50:151–155

Theander O, Westerlund EA (1986) Studies on dietary fiber. 3. improved procedures for analysis of dietary fiber. J Agric Food Chem 34:330–336

Toikka M, Brunow G (1999) Lignin-carbohydrate model compounds. Reactivity of methyl 3-*O*-(alpha-L-arabinofuranosyl)-beta-D-xylopyranoside and methyl beta-D-xylopyranoside towards a beta-*O*-4-quinone methide. J Chem Soc Perkin Trans 1:1877–1883

Toikka M, Sipilä J, Teleman A, Brunow G (1998) Lignin–carbohydrate model compounds. Formation of lignin–methyl arabinoside and lignin–methyl galactoside benzyl ethers via quinone methide intermediates. J Chem Soc Perkin Trans 1:3813–3818

Tokimatsu T, Umezawa T, Shimada M (1996) Synthesis of four diastereomeric lignin carbohydrate complexes (LCC) model compounds composed of a beta-0-4 lignin model linked to methyl beta-D-glucoside. Holzforschung 50:156–160

Yuan T, Sun S, Xu F, Sun R (2011) Characterization of lignin structures and lignin-carbohydrate complex (LCC) linkages by quantitative ^{13}C and 2D HSQC NMR spectroscopy. J Agric Food Chem 59:10604–10614

Zhang L, Gellerstedt G (2007) Quantitative 2D HSQC NMR determination of polymer structures by selecting suitable internal standard references. Magn Reson Chem 45:37–45

Zhang L, Gellerstedt G, Ralph J, Lu F (2006) NMR studies on the occurrence of spirodienone structures in lignins. J Wood Chem Technol 26:65–79